Chapter 3

Two-Dimensional Collocation Method for Generalized Partial Integro-Differential Equations of Fractional Order with Applications

3.1 Introduction

In the last decade, fractional derivatives and fractional integrals attracted many researchers due to their wide range of applications [11, 24, 66, 113, 114, 115]. Recently, some high-order approximations for PIDEFO were proposed and discussed. PIDEFO have many considerable applications in various fields [116, 117, 118, 119, 120, 121, 122, 123]. To solve the PIDEFO, several methods are developed by the authors in recent years. We cite here some of them. Dehghan and Abbaszadeh [124] solved two-dimensional weekly singular integro-differential equation based on

the finite element/finite difference method with error and convergence analysis. It was found that the scheme is unconditionally stable. In [125], authors developed direct meshless local Petrov–Galerkin (DMLPG) method to get the numerical solution of forth-order PDE in the defined domain. In [98], the authors present a new numerical scheme for solving neutral delay distributed-order fractional damped diffusion-wave equation. Here, the authors separate the time derivative by the finite element method, and the complete scheme is obtained by applying the spectral finite element method in the spatial direction. A new operational matrix method has been developed for finding numerical solutions to fractional-order differential equations in [65]. As we know, the theory of fractional integration and differentiation includes Riemann, Grunwald, Liouville, Leibnitz, and other derivatives therefore we define some new type of partial fractional derivatives which will help us to design a new type of PIDEFO. The recently proposed operators namely K and A/B operators are defined for the ordinary fractional derivative in [30]. We extend the theory of K and A/B operators in sense of partial fractional derivatives.

The K operator is defined for function $u(t,r)$ as follows

$$(K_P^{\gamma}u)(t,r) = p\int_a^t \omega_{\gamma}(s,r)u(s,r)ds + q\int_t^b \omega_{\gamma}(r,s)u(s,r)ds, \quad \gamma > 0. \tag{3.1}$$

Here, $t \in I = [a,b]$ and $P = (\gamma, a, b, p, q)$ is a set of parameters in which p, q are real constants. The kernel $\omega_{\gamma}(t,r)$ in K operator depends on γ. The K operator satisfies the linear property. For any $u_1(t,r)$ and $u_2(t,r)$ such that the right hand side of Eq. (3.1) exists then,

$$(K_P^{\gamma}(u_1+u_2))(t,r) = (K_P^{\gamma}u_1)(t,r) + (K_P^{\gamma}u_2)(t,r). \tag{3.2}$$

Now, we define B operator as,

$$(\mathcal{B}_P^{\gamma}u)_t(t,r) = \left(K_P^{m-\gamma}\left(\frac{\delta^m u}{\delta s^m}\right)\right)(t,r),$$
$$= p\int_a^t \omega_{m-\gamma}(s,r)\frac{\delta^m u(s,r)}{\delta s^m}ds + q\int_t^b \omega_{m-\gamma}(r,s)\frac{\delta^m u(s,r)}{\delta s^m}ds, \tag{3.3}$$

and

$$(\mathcal{B}_P^{\gamma}u)_r(t,r) = \left(K_P^{m-\gamma}\left(\frac{\delta^m u}{\delta s^m}\right)\right)(t,r),$$
$$= p\int_a^r \omega_{m-\gamma}(t,s)\frac{\delta^m u(t,s)}{\delta s^m}ds + q\int_r^b \omega_{m-\gamma}(s,t)\frac{\delta^m u(t,s)}{\delta s^m}ds, \tag{3.4}$$

where $m-1<\gamma<m$, m is a positive integer. We now define a new model of the PIDEFO as,

$$\sum_{i=1}^{R} d_i(t,r)(\mathcal{B}_P^{\gamma_i}u)(t,r) + \mathcal{H}(u(t,r)) = f(t,r). \tag{3.5}$$

Here, R is some fixed positive integer and $m_i-1<\gamma_i<m_i$ with m_i are some fixed positive integers, H is some linear or non-linear operator and $d_i(t,r)$ are some given functions. In Eq. (3.5), B operator has been taken in general (without subscript). The B operator can also be defined with respect to only t or r or in similar way. The Eq.(3.5) can have several forms depending on the choice of the kernel and the parameters a, b, p and q in B operator. For example, if we take $I=[0,1]$ and $p=1,\ q=0$ and $\omega_{(m-\gamma)}(t,r)=(t-r)^{(m-1-\gamma)}/(\Gamma(m-\gamma))$ in the B operator then this operator reduces to well-known Caputo fractional derivative. Similarly, other cases are also possible. Eq. (3.5) reduces to some well-known fractional models such as the following

1) Linear space-time fractional reaction-diffusion equation (FRDE)

Eq. (3.5) reduces to FRDE which is given by Eq. (3.6) for the particular choice of

variables $R = 2, d_1(t,r) = 1,\ d_2(t,r) = -b(r)$,

$$(\mathcal{B}_P^{\gamma_i} u)_t(t,r) + \mathcal{H}(u(t,r)) = f(t,r), \tag{3.6}$$

where $0 < \gamma_1 \leq 1 < \gamma_1 \leq 2$ and coefficient of diffusion, $b(r) > 0,\ (B_P^{(\gamma_1)}u)_t,\ (B_P^{(\gamma_2)}u)_r$ are given in Eq. (3.3) and (3.4) respectively.

2) Space-time fraction diffusion equations (STFDE) The space-time fractional diffusion equation (STFDE) [126], is obtained from Eq. (3.5) with substitution of $R = 1,\ d_1(t,r) = 1,\ d_2(t,r) = \mathcal{C},\ 0 < \gamma_1 = \gamma \leq 1,\ 1 < \gamma_1 = \gamma \leq 2$ in Eq. (3.5) and in Eq. (3.3), we take $p = 1, q = 0, \omega_{(m-\gamma)}(t,r) = (t-r)^{(m-1-\gamma)}/(\Gamma(m-\gamma))$. The STFDE given as,

$$\mathcal{D}_t^{\gamma} u(t,r) = \mathcal{C}\mathcal{D}_t^{\gamma} u(t,r), \tag{3.7}$$

with conditions

$$u(0,r) = g(r),\ r \in R,\ u(\mp\infty, t) = 0,\ t > 0, \tag{3.8}$$

where $\mathcal{D}_t^{\gamma} u(t,r) = \int_a^t \frac{(t-s)^{1-\gamma}}{\Gamma(2-\gamma)} \frac{\delta u(s,r)}{\delta s} ds = (\mathcal{B}_P^{\gamma} u)_t(t,r)$, $\mathcal{C}$ is fractional diffusion constant, $0 < \gamma \leq 1$ and $1 < \gamma \leq 2$, $u(x,t)$ is the (real) field variable, $\mathcal{D}_t^{\gamma}$ and $\mathcal{D}_t^{\gamma}$ are the Caputo time fractional and space fractional derivative of order γ with respect to t and r respectively, and $g(x)$ be a sufficiently well-behaved function.

3) Time fractional telegraph equations (TFTE)

We consider the Eq. (3.5) as,

$$d_1(t,r)(\mathcal{B}_P^{\gamma_1} u)(t,r) + \mathcal{H}(u(t,r)) = f(t,r),\ 0 < r < 1,\ t > 0. \tag{3.9}$$

Here, $(\mathcal{B}_P^{\gamma_1} u)(t,r)$ is the B operator defined above. Now if we put, $d_1(t,r) = 1, 1 < \gamma_1 < 2,\ p = 1,\ q = 0, \omega_{(m-\gamma)}(t,r) = (t-r)^{(m-1-\gamma)}/(\Gamma(m-\gamma))$, and

$$H(u(t,r)) = \frac{\delta u(t,r)}{\delta t} - \frac{\delta^2 u(t,r)}{\delta t^2}, \tag{3.10}$$

Eq. (3.9) reduces to the famous time fractional telegraph equations

$$\mathcal{D}_t^{\gamma} u(t,r) + \frac{\delta u(t,r)}{\delta t} - \frac{\delta^2 u(t,r)}{\delta t^2} = f(t,r),\ 0 < r < 1,\ t > 0. \tag{3.11}$$

These cases are studied in detail in Section 3.6. The motivation over here to consider this model is to put all such models together and develop a numerical method for its solution. This chapter is devoted to establish the connection with the existing models from the proposed model Eq. (3.5). The aim of the present chapter is to develop an accurate and efficient method for obtaining numerical solutions of various types of PIDEFOs. The proposed method is based on the collocation method with Jacobi polynomials as the basis functions. The next part of the chapter is arranged in the following way. In Section 3.2, we have provided some basic facts and properties of Jacobi polynomials that are needed to solve the problem. In Section 3.3, we have discussed the proposed method to solve PIDEFO. Further, Section 3.3 is divided into two parts, in the first part we have discussed the convergence analysis and in the second part, the error analysis is presented. In Section 3.6, we have shown three applications of the proposed model. Two examples based on the problem are discussed in Section 3.7 with variations in parameters. Finally, in Section 3.8, the findings are concluded.

3.2 Preliminaries

In this section, we describe some basics of Jacobi polynomials which will be used throughout the chapter. The Jacobi polynomial $j_{a,b}^N(r)$ [127, 1] defined as,

$$j_{a,b}^N(r) = \sum_m \binom{N+a}{m} \binom{N+b}{N-m} \left(\frac{r-1}{2}\right)^{N-m} \left(\frac{r+1}{2}\right)^m,\ N \geq m \geq 0, \tag{3.12}$$

or

$$j_{a,b}^{N}(r) = \frac{\Gamma(a+N+1)}{N!\Gamma(a+b+N+1)} \sum_{i=0}^{j} \binom{N}{i} \frac{\Gamma(a+b+N+i+1)}{\Gamma(a+i+1)} \left(\frac{r-1}{2}\right)^{i}, \quad (3.13)$$

Jacobi polynomials up to degree N form the orthogonal basis over $[-1,1]$. Orthogonality of Jacobi polynomials $j_{(a,b)}^{N}(r)$ on the interval $[-1,1]$ is defined by,

$$< j_{a,b}^{N}(r) | j_{a,b}^{M}(r) >_S = \frac{2^{a+b+1}}{2N+a+b+1} \frac{(N+a)!(N+b)!}{N!(N+a+b)!} \delta_{NM},\ a,b,a+b > -1, \quad (3.14)$$

where,δ_{NM} is Kronecker Delta function. Here, $< .|. >_S$ denotes the weighted inner product with respect to weight function $S(r) = (1-r)^a(1+r)^b$ and the corresponding norm is defined by

$$\|j_{a,b}^{N}(r)\|_S = (< j_{a,b}^{N}(r) | j_{a,b}^{N}(r) >_S)^{1/2} = \left(\int_{-1}^{1} (j_{a,b}^{N}(r))^2 S(r)\, dr \right)^{1/2}. \quad (3.15)$$

3.3 Two-Dimensional Collocation Method for PIDEFO

In this section, we extend the collocation method described to solve the PIDEFO given by Eq. (3.5). We choose a function from a finite dimensional family of functions supposed to be the best approximation of the exact solution. Then, we choose some collocation points from the domain to convert the model into a set of algebraic equations. After solving this set of equations, we get the approximate solution. In the proposed method, we approximate the solution in form of linear combination with basis function as the product of Jacobi polynomials. Let

$u_{NM} = u_{00}, u_{01}, u_{02}, \ldots, u_{0M}, u_{10}, u_{11}, u_{12}, \ldots, u_{1M}, u_{N0}, u_{N1}, u_{N2}, \ldots, u_{NM}$ be a finite dimensional basis, where,

$$u_{ij}(t,r) = j^i_{a,b}(2t-1)j^j_{a,b}(2r-1). \tag{3.16}$$

We assume the solution in the form,

$$u(t,r) = \sum_{i=0}^{\infty}\sum_{j=0}^{\infty} a_{ij}u_{ij}(t,r) = \sum_{i=0}^{\infty}\sum_{j=0}^{\infty} a_{ij}j^i_{a,b}(2t-1)j^j_{a,b}(2r-1). \tag{3.17}$$

In this expansion, we shift the Jacobi polynomials $j^N_{a,b}$ and weight function S from $[-1,1]$ to $[0,1]$ using a transformation $x \to 2x-1$. Here the coefficients a_{ij} are unknown, $j^j_{a,b}(2r-1)$ and $j^i_{a,b}(2t-1)$ denote the shifted Jacobi polynomials respectively. From Eq. (3.17), we have,

$$\begin{aligned} a_{ij} = &\left(\frac{1}{\|j^j_{a,b}(2r-1)\|_{S(2r-1)}\|j^i_{a,b}(2t-1)\|_{S(2t-1)}}\right)^2 \\ &\times \int_0^1\int_0^1 B(t,r)j^j_{a,b}(2r-1)S(2r-1)j^i_{a,b}(2t-1)S(2t-1)\,dr\,dt. \end{aligned} \tag{3.18}$$

Truncating the infinite series in Eq. (3.17), $u(t,r)$ can be approximated as,

$$u_{NM}(t,r) = \sum_{i=0}^{N}\sum_{j=0}^{M} a_{ij}u_{ij}(t,r) = \sum_{i=0}^{N}\sum_{j=0}^{M} a_{ij}j^i_{a,b}(2t-1)j^j_{a,b}(2r-1). \tag{3.19}$$

Now, we substitute the value of $u_{NM}(t,r)$ from Eq. (3.19) in Eq. (3.5) which gives,

$$\begin{aligned} \sum_{i=1}^{R} d_i(t,r)(\mathcal{B}^{\gamma_i}_P u_{NM})(t,r) + \mathcal{H}(u_{NM}(t,r)) &= f(t,r), \\ \sum_{i=0}^{N}\sum_{j=0}^{M} a_{ij}\sum_{i=1}^{R}\left(d_i(t,r)\left((\mathcal{B}^{\gamma_i}_P u_{ij})(t,r)\right)\right) + \mathcal{H}\left(\sum_{i=0}^{N}\sum_{j=0}^{M} a_{ij}\sum_{j=0}^{M} a_{ij}u_{ij}(t,r)\right) &= f(t,r). \end{aligned} \tag{3.20}$$

After solving and rearranging the terms, we rewrite Eq. (3.20) in the following manner,

$$\mathcal{C}(i,j,t,r) = f(t,r). \tag{3.21}$$

In Eq. (3.21),

$$\mathcal{C}(i,j,t,r) = \sum_{i=0}^{N}\sum_{j=0}^{M} a_{ij} \sum_{i=1}^{R} \left(d_i(t,r)\left((\mathcal{B}_P^{\gamma_i} u_{ij})(t,r)\right)\right) + \mathcal{H}\left(\sum_{i=0}^{N}\sum_{j=0}^{M} a_{ij} \sum_{j=0}^{M} a_{ij} u_{ij}(t,r)\right). \tag{3.22}$$

Collocating Eq. (3.21) at collocation points (t_{Ni}, r_{Mj}) as the roots of $M+1$ and $N+1$ shifted Jacobi polynomials respectively. We obtain the following set of equations,

$$\mathcal{C}(i,j,t_{Ni},r_{Mj}) = f(t_{Ni},r_{Mj}),\ 0 \le i \le N,\ 0 \le j \le M. \tag{3.23}$$

Eq. (3.23) is a system of algebraic equations and by solving it for a_{ij}, the approximate value of a_{ij} can be obtained. If H is nonlinear, Eq. (3.23) is a nonlinear system of equations which can be solved by Newton's iterative method. Thus, we obtained the approximate value of $B(t,r)$.

3.4 Convergence Analysis

Theorem 3.4.1. Suppose $u(t,r)$ be smooth sufficiently and $u_{NM}(t,r)$ denote the Jacobi polynomial approximation of $u(t,r)$. And, if $|u(t,r)| \le M$, then $u_{NM}(t,r)$ converges to $u(t,r)$ uniformly. Moreover,

$$|u(t,r) - u_{NM}(t,r)| \to 0 \text{ as } N, M \to \infty.$$

Proof: From Eq. (3.17) and (3.19), we have

$$
\begin{aligned}
u(t,r) - u_{NM}(t,r) = & \sum_{i=M+1}^{\infty} \sum_{j=0}^{\mathcal{M}} a_{i,j} j_{a,b}^{i}(2t-1) j_{a,b}^{j}(2r-1) \\
& + \sum_{i=N+1}^{\infty} \sum_{j=M+1}^{\infty} a_{i,j} j_{a,b}^{i}(2t-1) j_{a,b}^{j}(2r-1) \\
& + \sum_{i=0}^{N} \sum_{j=M+1}^{\infty} a_{i,j} j_{a,b}^{i}(2t-1) j_{a,b}^{j}(2r-1),
\end{aligned} \tag{3.24}
$$

which implies,

$$
\begin{aligned}
& \|u(r,t) - u_{N,M}(r,t)\|^2 \\
& = \left\| \sum_{i=N+1}^{\infty} \sum_{j=0}^{M} a_{ij} j_{a,b}^{i}(2t-1) j_{a,b}^{j}(2r-1) + \sum_{i=N+1}^{\infty} \sum_{j=M+1}^{\infty} a_{ij} j_{a,b}^{i}(2t-1) j_{a,b}^{j}(2r-1) \right. \\
& \left. + \sum_{i=0}^{N} \sum_{j=M+1}^{\infty} a_{ij} j_{a,b}^{i}(2t-1) j_{a,b}^{j}(2r-1) \right\|^2, \\
& \leq \sum_{i=N+1}^{\infty} \sum_{j=0}^{M} a_{ij}^2 \left(\|j_{a,b}^{j}(2r-1)\|_{S(2r-1)} \right)^2 \left(\|j_{a,b}^{i}(2t-1)\|_{S(2t-1)} \right)^2 \\
& + \sum_{i=N+1}^{\infty} \sum_{j=M+1}^{\infty} a_{ij}^2 \left(\|j_{a,b}^{j}(2r-1)\|_{S(2r-1)} \right)^2 \left(\|j_{a,b}^{i}(2t-1)\|_{S(2t-1)} \right)^2 \\
& + \sum_{i=0}^{N} \sum_{j=M+1}^{\infty} a_{ij}^2 \left(\|j_{a,b}^{j}(2r-1)\|_{S(2r-1)} \right)^2 \left(\|j_{a,b}^{i}(2t-1)\|_{S(2t-1)} \right)^2 \|^2.
\end{aligned} \tag{3.25}
$$

From Eq. (3.18), we have,

$$
\begin{aligned}
a_{ij} = & \left(\frac{1}{\|j_{a,b}^{j}(2r-1)\|_{S(2r-1)} \|j_{a,b}^{i}(2t-1)\|_{S(2t-1)}} \right)^2 \\
& \times \int_0^1 |B(t,r) j_{a,b}^{j}(2t-1) S(2t-1) dt| \int_0^1 j_{a,b}^{i} S(2r-1)\, dr|.
\end{aligned} \tag{3.26}
$$

Now we apply a change of variable $r = (y+1)/2$, in the second integral, we obtain

$$a_{ij} = 2\left(\frac{1}{\|j^j_{a,b}(2r-1)\|_{S(2r-1)}\|j^i_{a,b}(2t-1)\|_{S(2t-1)}}\right)^2 \times \int_0^1 \sup_{r\in[0,1]} |B(t,r)j^j_{a,b}(2t-1)S(2t-1)dt| \int_{-1}^1 j^i_{a,b}(y)S(y)\, dy|. \tag{3.27}$$

Substitute the value of $j^i_{(a,b)}(y)$ and $S(y)$,

$$a_{ij} \leq 2\left(\frac{1}{\|j^j_{a,b}(2r-1)\|_{S(2r-1)}\|j^i_{a,b}(2t-1)\|_{S(2t-1)}}\right)^2 \int_0^1 \sup_{r\in[0,1]} |B(t,r)j^j_{a,b}(2t-1)S(2t-1)dt| \sum_{k=0}^{i} A(k,a,b,i) \int_{-1}^1 |(1-y)^\gamma(1+y)^\gamma \left(\frac{y-1}{2}\right)^k |\, dy. \tag{3.28}$$

Here, $A(k,a,b,i) = \binom{(i)}{k}\frac{\Gamma(a+i+1)}{i!\Gamma(a+b+i+1)}\frac{\Gamma(a+b+i+k+1)}{\Gamma(a+k+1)}$.

$$a_{ij} \leq 2\left(\frac{1}{\|j^j_{a,b}(2r-1)\|_{S(2r-1)}\|j^i_{a,b}(2t-1)\|_{S(2t-1)}}\right)^2 \int_0^1 \sup_{r\in[0,1]} |u(t,r)j^j_{a,b}(2t-1)S(2t-1)dt| \sum_{k=0}^{i} A(k,a,b,i)\left(\frac{1}{2}\right)^k \int_{-1}^1 |(1-y)^{\gamma+k}(1+y)^b|\, dy. \tag{3.29}$$

Now,

$$\int_{-1}^1 |(1-y)^{\gamma+k}(1+y)^b|\, dy = 2\frac{\Gamma(a+k+1)\Gamma(b+1)}{\Gamma(a+b+k+2)}. \tag{3.30}$$

Using Eq. (3.30) and substituting the values of $A(k,a,b,i)$ and $\|j^j_{a,b}(2r-1)\|_{S(2r-1)}$ in Eq. (3.29), we obtain,

$$a_{ij} \leq \frac{1}{2^{a+b+i-1}} \frac{(2i+a+b+1)\Gamma(b+1)}{\Gamma(i+b+1)} \left(\frac{1}{\|j^i_{a,b}(2t-1)\|_{S(2t-1)}} \right)^2 \\ \left| \int_0^1 \sup_{r\in[0,1]} |B(t,r)| j^i_{a,b}(2t-1) S(2t-1) dt \right|. \tag{3.31}$$

Repeating the same procedure for the second integral, we obtain

$$a_{ij} \leq \frac{1}{2^{a+b+i-1}} \frac{(2i+a+b+1)\Gamma(b+1)}{\Gamma(i+b+1)} \frac{1}{2^{a+b+j-1}} \frac{(2j+a+b+1)\Gamma(b+1)}{\Gamma(j+b+1)} \sup_{r\in[0,1]} |u(t,r)|. \tag{3.32}$$

Now, from Eqs. (3.15), (3.25) and (3.32), we have

$$\|u(t,r) - u_{NM}(t,r)\| \leq A(a,b,N,M), \tag{3.33}$$

where,

$$\begin{aligned} A(a,b,N,M) = & \sum_{i=N+1}^{\infty} \sum_{j=M+1}^{\infty} \frac{1}{2^{a+b+2i-3}} \frac{(2i+a+b+1)(\Gamma(b+1)^2)\Gamma(i+a+1)}{i!\Gamma(i+b+1)\Gamma(i+a+b+1)} \\ & \frac{1}{2^{a+b+2j-3}} \frac{(2j+a+b+1)(\Gamma(b+1)^2)\Gamma(j+a+1)}{j!\Gamma(j+b+1)\Gamma(j+a+b+1)} \\ & + \sum_{i=0}^{N} \sum_{j=M+1}^{\infty} \frac{1}{2^{a+b+2i-3}} \frac{(2i+a+b+1)(\Gamma(b+1)^2)\Gamma(i+a+1)}{i!\Gamma(i+b+1)\Gamma(i+a+b+1)} \\ & \frac{1}{2^{a+b+2j-3}} \frac{(2j+a+b+1)(\Gamma(b+1)^2)\Gamma(j+a+1)}{j!\Gamma(j+b+1)\Gamma(j+a+b+1)} \\ & + \sum_{i=N+1}^{\infty} \sum_{j=0}^{M} \frac{1}{2^{a+b+2i-3}} \frac{(2i+a+b+1)(\Gamma(b+1)^2)\Gamma(i+a+1)}{i!\Gamma(i+b+1)\Gamma(i+a+b+1)} \\ & \frac{1}{2^{a+b+2j-3}} \frac{(2j+a+b+1)(\Gamma(b+1)^2)\Gamma(j+a+1)}{j!\Gamma(j+b+1)\Gamma(j+a+b+1)}, \end{aligned} \tag{3.34}$$

is the square root of the right side term of Eq. (3.34). Since, both series in the

product on right hand side of Eq. (3.34) are converges absolutely to 0, we have, $|u(t,r) - u_{NM}(t,r)| \to 0$ as $N, M \to \infty$.

3.5 Error Analysis

Theorem 3.5.1. Let $(B_P^\gamma u_{NM})_t(t,r)$ be the approximation of $(B_P^\gamma u)_t(t,r)$ and $u(t,r)$ be m-times continuously differential function with respect to t and r i.e., $u(t,r) \in C^m$. Assume that, $\omega_\gamma(t,r)$ be square summable kernel i.e., there exists a positive real number Ω such that,

$$\int_0^1 \int_0^1 (\omega_\gamma(t,r))^2 \, dt \, dr \leq \Omega^2, \tag{3.35}$$

then,

$$\|(B_P^\gamma u)_t(t,r) - (B_P^\gamma u_{NM})_t(t,r)\| \leq (|p|\Omega + |q|\Omega) A(a,b,N,M). \tag{3.36}$$

Proof We have,

$$\begin{aligned}
&(B_P^\gamma u)_t(t,r) - (B_P^\gamma u_{NM})_t(t,r) \\
&= \left(p \int_a^t \omega_\gamma(s,r) \frac{\delta^m u(s,r)}{\delta s^m} ds + q \int_t^b \omega_\gamma(r,s) \frac{\delta^m u(s,r)}{\delta s^m} ds \right) \\
&- \left(p \int_a^t \omega_\gamma(s,r) \frac{\delta^m u_{NM}(s,r)}{\delta s^m} ds + q \int_t^b \omega_\gamma(r,s) \frac{\delta^m u_{NM}(s,r)}{\delta s^m} ds \right), \\
&= p \int_a^t \omega_\gamma(s,r) \frac{\delta^m (u(s,r) - u_{NM}(s,r))}{\delta s^m} ds + q \int_t^b \omega_\gamma(r,s) \frac{\delta^m (B(s,r) - u_{NM}(s,r))}{\delta s^m} \, ds,
\end{aligned} \tag{3.37}$$

$$\|(B_P^{\gamma}u)_t(t,r) - (B_P^{\gamma}u_{NM})_t(t,r)\| \leq \|p\int_a^t \omega_{\gamma}(s,r)\frac{\delta^m(u(s,r)-u_{NM}(s,r))}{\delta s^m}ds\| + \|q\int_t^b \omega_{\gamma}(r,s)\frac{\delta^m(u(s,r)-u_{NM}(s,r))}{\delta s^m}\,ds\|. \tag{3.38}$$

Since $u(t,r),\ u_{NM}(s,r) \in \mathcal{C}^m$, the right hand side term of Eq. (3.38) term is bounded. Moreover,

$$\begin{aligned}&\|(B_P^{\gamma}u)_t(t,r) - (B_P^{\gamma}u_{NM})_t(t,r)\|\\ &\leq |p|\Omega\|u(t,r)-u_{NM}(t,r)\| + |q|\Omega\|u(t,r)-u_{NM}(t,r)\|, \qquad (3.39)\\ &\|(B_P^{\gamma}u)_t(t,r) - (B_P^{\gamma}u_{NM})_t(t,r)\|\\ &\leq (|p|\Omega + |q|\Omega)\|u(t,r)-u_{NM}(t,r)\|. \qquad (3.40)\end{aligned}$$

Using Eq. (3.33), we get,

$$\|(B_P^{\gamma}u)_t(t,r) - (B_P^{\gamma}u_{NM})_t(t,r)\|(|p|\Omega + |q|\Omega)A(a,b,N,M). \tag{3.41}$$

3.6 Applications of The PIDEFO

Here, we discuss the special cases of the presented model of PIDEFO and also present an approach to solve it using collocation method with Jacobi polynomials. The PIDEFO reduces to 1) linear space-time fractional reaction-diffusion equation (FRDE), 2) space-time fraction diffusion equations (STFDE) and 3) time fractional telegraph equations (TFTE) in a particular case. These three problems are discussed below.

3.6.1 Linear Space-Time Fractional Reaction-Diffusion Equations in Sense of B Operator

We define linear space-time fractional reaction-diffusion equation (FRDE) on $0 < x < 1,\ t > 0$ in terms of B operator with $0 < \gamma_1 \leq 1$ and $1 < \gamma_2 \leq 2$ as,

$$(B_P^{(\gamma_1)}u)_t(t,r) = b(r)(B_P^{(\gamma_2)}u)_r(t,r) + H(u(t,r)) + f(t,r), \tag{3.42}$$

where the coefficient of diffusion, $b(r) > 0, (B_P^{(\gamma_1)}u)_t, (B_P^{(\gamma_2)}u)_r$ are defined by Eq. (3.3) and (3.4) respectively. The Eq. (3.42) is the special case of the Eq. (3.5) for $R = 2,\ d(t,r) = 1,\ d_2(t,r) = -b(r)$. Now, if we set the parameters in B operator as $= 0, b = 1, p = 1, q = 0, \omega_{(m-\gamma)}(t,r) = (t-r)^{(m-1-\gamma)}/(\Gamma(m-\gamma))$, and if $0 < \gamma_1 \leq 1 < \gamma_2 \leq 2$, then $(B_P^{(\gamma_1)}u)_t$ and $(B_P^{(\gamma_2)}u)_r$ reduce to the standard Caputo time and space derivatives respectively, defined by,

$$(B_P^{(\gamma_1)}u)_t(t,r) = \int_a^t \frac{(r-s)^{-\gamma_1}}{\Gamma(1-\gamma_1)} \frac{\delta u(s,r)}{\delta s}\, ds = \mathcal{D}_t^{-\gamma_1}u(t,r), \tag{3.43}$$

and

$$(B_P^{(\gamma_2)}u)_r(t,r) = \int_a^r \frac{(r-s)^{-\gamma_2}}{\Gamma(2-\gamma_2)} \frac{\delta^2 u(t,s)}{\delta s^2}\, ds = \mathcal{D}_r^{-\gamma_2}u(t,r). \tag{3.44}$$

Under these settings, Eq. (3.42) converts into the famous FRDE,

$$\mathcal{D}_t^{\gamma_1}u(t,r) = b(r)\mathcal{D}_r^{\gamma_2}u(t,r) + H(u(t,r)) + f(t,r). \tag{3.45}$$

Now, we take, $H(u(t,r)) = c(r)u(t,r)$, where $c(r) > 0$, Eq. (3.45) is known linear FRDE [128] and if $H(u(t,r))$ is a nonlinear function then it is called nonlinear FRDE. In nonlinear FRDE, $H(u(t,r))$ is a non-linear reaction term which models the population growth. For example, a typical choice is Fisher's equation

$H(u(t,r)) = gu(t,r)(1-u(t,r))/C$, where g is the intrinsic growth rate and C the carrying capacity. For solving Eq. (3.45), it is sufficient to develop a method for Eq. (3.5) as Eq. (3.45) is a particular case of Eq. (3.5).

3.6.2 Space-Time Fractional Diffusion Equation in Sense of B Operator

We consider the diffusion equation [126] known as the space-time fractional diffusion equation (STFDE), is given by,

$$\mathcal{D}_t^{\gamma} u(t,r) = \mathcal{C}\mathcal{D}_r^{\gamma} u(t,r), \tag{3.46}$$

with conditions, $u(0,r) = g(r), r \in R$, $u(\infty,t) = 0$, $t > 0$, where the positive constant C is fractional diffusion coefficient, $0 < \gamma \leq 1$ and $1 < \gamma \leq 2$, $u(x,t)$ is the (real) field variable, $\mathcal{D}_t^{\gamma}$ is the Caputo time fractional derivative of order γ with respect to t, and $\mathcal{D}_r^{\gamma}$ is also Caputo space fractional derivative of order γ with respect to r, and $g(x)$ be a sufficiently well-behaved function. The fractional diffusion equation (3.46) is important for the study of the mechanism of anomalous diffusion of the transport processes through complex systems with fractal media. Eq. (3.46) can be easily derived from Eq. (3.5). For this we take $R = 1$, $d_1(t,r) = -\mathcal{C}$, $0 < \gamma_1 = \gamma \leq 1$, $1 < \gamma_1 = \gamma \leq 2$ and in Eq. (3.3), we take $p = 1$, $q = 0$, $\omega_{(m-\gamma)}(t,r) = (t-r)^{(m-1-\gamma)}/(\Gamma(m-\gamma))$. We get,

$$\mathcal{D}_t^{\gamma} u(t,r) = \int_a^t \frac{(t-s)^{1-\gamma}}{\Gamma(2-\gamma)} \frac{\delta u(s,r)}{\delta s}\, ds = (\mathcal{B}_P^{\gamma} u)_t(t,r), \tag{3.47}$$

For $\mathcal{D}_t^{\gamma} u(t,r)$ we use the definition Eq. (3.4) of $\mathcal{B}$ operator

$$\mathcal{D}_r^{\gamma} u(t,r) = \int_a^r \frac{(r-s)^{1-\gamma}}{\Gamma(2-\gamma)} \frac{\delta^2 u(t,s)}{\delta s^2}\, ds = (\mathcal{B}_P^{\gamma} u)_r(t,r). \tag{3.48}$$

3.6.3 Time Fractional Telegraph Equation

We consider Eq. (3.5) as,

$$d_1(t,r)(\mathcal{B}_P^{\gamma_1} u)(t,r) + \mathcal{H}(u(t,r)) = f(t,r),\ 0 < r < 1,\ t > 0. \tag{3.49}$$

Here, $(\mathcal{B}_P^{\gamma_1} u)(t,r)$ is the B operator defined above. Now if we take, $d_1(t,r) = 1,\ 1 < \gamma_1 < 2,\ p = 1,\ q = 0,\ \omega_{(m-\gamma)}(t,r) = (t-r)^{(m-1-\gamma)}/(\Gamma(m-\gamma))$, and

$$\mathcal{H}(u(t,r)) = \frac{\delta u(t,r)}{\delta t} - \frac{\delta^2 u(t,r)}{\delta t^2}, \tag{3.50}$$

Eq. (3.49) reduces to the famous time fractional telegraph equations

$$\mathcal{D}_t^{\gamma} u(t,r) + \frac{\delta u(t,r)}{\delta t} - \frac{\delta^2 u(t,r)}{\delta t^2} = f(t,r),\ 0 < r < 1,\ t > 0. \tag{3.51}$$

Thus, it can be observed that several fractional order models can be deduced by Eq. (3.5) or in other words, Eq. (3.5) can be considered as the generalized form of these equations. This was motivation to put all such equations in one form and develop a solution method for this new model. The test examples based on these models and their approximate solution using the discussed method will now be presented.

3.7 Numerical Examples

Here, we consider the test examples based on the three models discussed in the previous section. We consider test examples with known exact solutions and also discuss a case of the proposed model for which the exact solution is not known. The stability of the method is also shown. The accuracy of the proposed method is demonstrated by the maximum absolute error, defined as
$E = |u(t,r) - u_{NM}(t,r)|$, where, $u(t,r)$ and $u_{NM}(t,r)$ denote the exact and numerical solution respectively.

Example 3.7.1. We consider an example of the form,

$$(\mathcal{B}_P^{\gamma_1} u)(t,r) - b(r)(\mathcal{B}_P^{\gamma_2} u)(t,r) + c(r)u(t,r) = f(t,r), \tag{3.52}$$

where, $b(r) = \Gamma(1.2)r^{1.8}$, $c(r) = 2$, $f(t,r) = 3(4t^2+1)r^3 + 32/(3\sqrt{\pi})t^{1.5}(r^2 - r^3)$, and with the initial and boundary conditions,

$$u(t,0) = u_r(t,0) = 0, \tag{3.53}$$

$$u(0,r) = (r^2 - r^3). \tag{3.54}$$

The model given by Eq. (3.52) can be written in form of Eq. (3.5) with, $d_1(t,r) = 1, d_2(t,r) = b(r), H(u(t,r)) = c(r)u(t,r)$, and B operator with $= 1, q = 1$, $\omega_{(m-\gamma)}(t,r) = (t-r)^{(m-1-\gamma)}/(\Gamma(m-\gamma))$. This equation is solved for $\gamma_1 = 0.5$ and $\gamma_2 = 1.8$ using Jacobi collocation method. To solve this problem, we combine Eq. (3.53) with the initial condition given by Eq. (3.54) as,

$$(\mathcal{B}_P^{\gamma_1} u)(t,r) - b(r)(\mathcal{B}_P^{\gamma_2} u)(t,r) + c(r)u(t,r) - u(0,r) = f(t,r) - (r^2 - r^3). \tag{3.55}$$

We solve this Eq. (3.55) with different values of M and N and obtained numerical results are presented in Table (3.1). Now, if we choose $p = 1,\ q = 0$, Eq. (3.55) reduces to linear space-time fractional reaction-diffusion equations (Section 4.1) so,

$$\mathcal{D}_t^{\gamma_1} u(t,r) - b(r)\mathcal{D}_r^{\gamma_2} u(t,r) + c(r)u(t,r) = f(t,r) - (r^2 - r^3) + u(0,r). \tag{3.56}$$

Here, $\mathcal{D}_t^{\gamma_1} u(t,r)$ is the Caputo time-fractional derivative of order $0 < \gamma_1 < 1$, defined by,

$$\mathcal{D}_t^{\gamma_1} u(t,r) = \frac{1}{\Gamma(1-\gamma_1)} \int_0^t (t-s)^{-\gamma_1} \frac{\delta u(s,r)}{\delta s}\, ds, \tag{3.57}$$

for $0 < \gamma_1 < 1$, and for $\gamma_1 = 1$ given by Eq. (3.58)

$$\mathcal{D}_t^{\gamma_1} u(t,r) = \frac{\delta u(t,r)}{\delta t}. \tag{3.58}$$

$\mathcal{D}_r^{\gamma_2} u(t,r)$ is the Caputo space-fractional derivative of order $1 < \gamma_2 \leq 2$, defined by,

$$\mathcal{D}_t^{\gamma_2} u(t,r) = \frac{1}{\Gamma(2-\gamma_2)} \int_0^t (t-s)^{1-\gamma_2} \frac{\delta^2 u(s,r)}{\delta s^2}\, ds, \tag{3.59}$$

for $1 < \gamma_2 < 2$, and for $\gamma_2 = 2$ given by Eq. (3.60)

$$\mathcal{D}_t^{\gamma_2} u(t,r) = \frac{\delta^2 u(t,r)}{\delta t^2}. \tag{3.60}$$

For, $\gamma_1 = 0.5, \gamma_2 = 1.8$, the exact solution of Eq. (3.56) is $(4t^2 + 1)(r^2 - r^3)$. We calculate the approximate solution of Eq. (3.56) with $N = 2, M = 3$. The absolute errors are given in Table (3.2) and $L_2,\ L_\infty$ errors are presented in Table (3.3). Fig. 3.1 represents the absolute error between the exact and the numerical solutions. It is clear from the numerical results that approximate solution has well agreement with the exact solution.

3.7.1 Effect of Collocating at Equally-Spaced Points

1. Boundary points exclusive: If, instead of collocating at zeros of Jacobi polynomials, the collocation points are determined by the use of,

$t_{Ni} = i/(N+2), \quad i = 1, 2, 3, \ldots N+1,$

$r_{Mj} = j/(M+2), \quad j = 1, 2, 3 \ldots M+1.$

TABLE 3.1: Numerical solution for different values of M and N for Example (3.7.1).

M	N	Numerical solution of $B_{NM}(t,r)$
1	1	0.134577-0.114777t-1.364984r+tr
	2	-0.022413+0.055932t-0.1217792t^2+0.0075076r -0.4206833tr+t^2r
	3	0.0134+0.0033t-0.321r-0.00192tr -0.7401r2+1.7875tr^2+1.01294r^3+tr^3
2	1	-0.01089-0.01121t+0.15094r +0.173983tr+0.712688r^2+tr^2
	2	-0.18898-0.00148t-0.1017577t^2+2.6578r + 0.1775tr +1.4471t^2r+7.2434r^2+9.9493tr^2+t^2r^2
	3	0.0102-0.0032t+0.0063-0.2083r+ 0.059tr -0.0974-0.609r^2+0.431tr^2-0.265t^2r^2 +0.546r^3 +0.19599tr^3+t^2r^3

TABLE 3.2: AE for Example (3.7.1).

(t,r)	$N=2,\ M=3$
(0.1,0.1)	4.614×10^{-15}
(0.2,0.2)	2.101×10^{-14}
(0.3,0.3)	4.843×10^{-14}
(0.4,0.4)	8.723×10^{-14}
(0.5,0.5)	1.343×10^{-13}
(0.6,0.6)	1.822×10^{-13}
(0.7,0.7)	2.174×10^{-13}
(0.8,0.8)	1.605×10^{-13}
(0.9,0.9)	3.330×10^{-15}
(1.0,1.0)	5.109×10^{-14}

In this technique, we choose the equally-spaced collocation points without boundary points (in this case we omit 0 and 1). Taking these collocation points, we solve Eq. (3.56) with $N = M = 3$ and obtained absolute errors are listed in Table (3.4).

TABLE 3.3: L_2 and L_∞ errors for Example (3.7.1).

Errors	$N = 2,\ M = 2$
L_2 errors	4.278×10^{-13}
L_∞ errors	2.196×10^{-13}

2. Boundary points inclusive In this technique, we choose the collocation points,

$t_{Ni} = i/(N+1), \quad i = 1, 2, 3, \ldots N+1,$

$r_{Mj} = j/(M+1), \quad j = 1, 2, 3 \ldots M+1.$

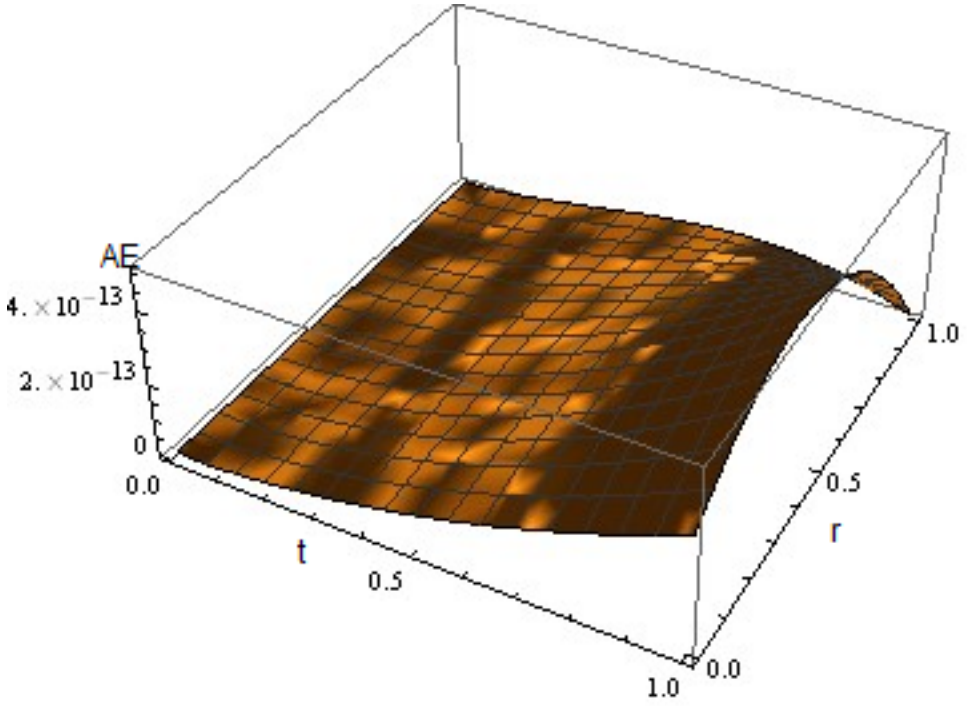

FIGURE 3.1: Plot of absolute numerical error for Eq. (3.56) for $N = 2,\ M = 3$.

Here, we include only right boundary, which is 1, in choosing the collocation points since at left boundary the Eq. (3.56) becomes meaningless. Using these points with $N = M = 3$, we calculated the numerical solution of Eq. (3.56) and obtained

TABLE 3.4: Comparison of different collocation points with $N = M = 3$ for Example (3.7.1).

(t,r)	Points at zeros	Without boundary	With boundary
(0,0)	1.242×10^{-15}	4.211×10^{-15}	2.603×10^{-14}
(0.1,0.1)	5.620×10^{-16}	5.953×10^{-15}	1.158×10^{-15}
(0.2,0.2)	2.081×10^{-16}	2.765×10^{-14}	3.835×10^{-14}
(0.3,0.3)	1.221×10^{-15}	6.429×10^{-14}	9.901×10^{-14}
(0.4,0.4)	2.775×10^{-15}	1.200×10^{-13}	1.849×10^{-13}
(0.5,0.5)	5.495×10^{-15}	2.091×10^{-13}	2.987×10^{-13}
(0.6,0.6)	1.010×10^{-14}	3.677×10^{-13}	4.419×10^{-13}
(0.7,0.7)	1.759×10^{-14}	6.701×10^{-13}	6.1170×10^{-13}
(0.8,0.8)	2.942×10^{-14}	1.248×10^{-12}	8.279×10^{-13}
(0.9,0.9)	4.757×10^{-14}	2.312×10^{-12}	1.083×10^{-12}
(1.0,1.0)	7.427×10^{-14}	4.179×10^{-12}	1.394×10^{-12}

absolute errors are shown in Table (3.4). In accordance with established facts (Table (3.4)), it is clearly observed from the results produced that these points are valid for collocation method via Legendre polynomial as trial functions. Errors accrued with each set of points are also minimal that these can be functionally applied in practical setting. A further study of these results, points at zeros of Legendre polynomial performed better. To test the accuracy of the proposed method, we obtain the numerical solution for different values of γ_1 and γ_2. The numerical solution for different values of γ_1 and γ_2 are shown in Figs. (3.2-3.4) and Figs. (3.5-3.7), respectively. It can be observed that the approximate solution approaches to the exact solution as γ_1 and γ_2 approaches to 0.5 and 1.8 respectively. It is clear from the Figs. (3.4-3.6) that numerical solutions converge to exact solution as the value γ_1 tends to 0.5.

$$\sum_{i=1}^{R} d_i(t,r)(\mathcal{B}_P^{\gamma_i} u)(t,r) + \mathcal{H}(u(t,r)) = f(t,r) + \epsilon\delta. \tag{3.61}$$

Let $u_{NM}^{\delta}(t,r)$ denote the approximate solution of Eq. (3.61) with noise term $\epsilon\delta$ where, ϵ is a sufficiently small constant and δ is a uniform random variable in interval

$[-1, 1]$. We denote the approximate solution of Eq. (3.61) under

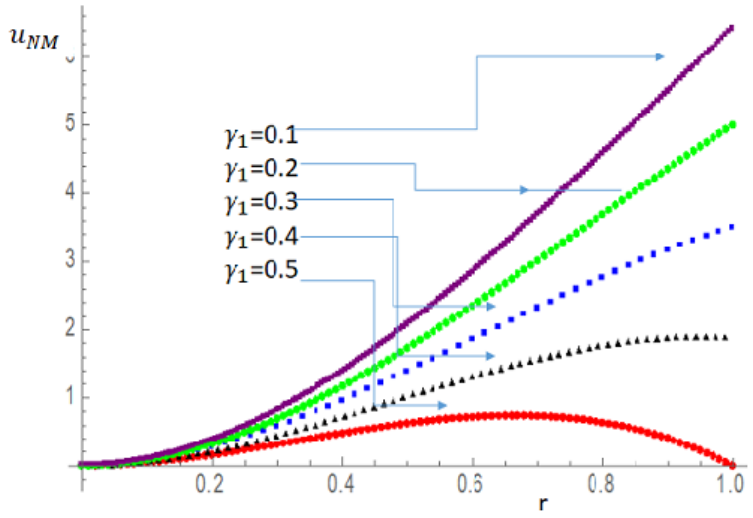

FIGURE 3.2: Numerical solution for different values of γ_1 for Equation Eq. (3.56) at $t = 1$.

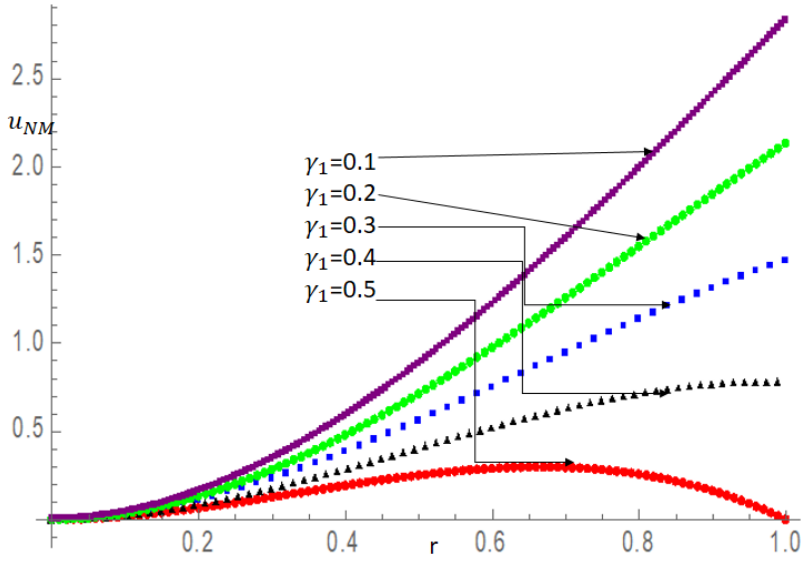

FIGURE 3.3: Numerical solution for different values of γ_1 for Equation Eq. (3.56) at $t = 0.5$.

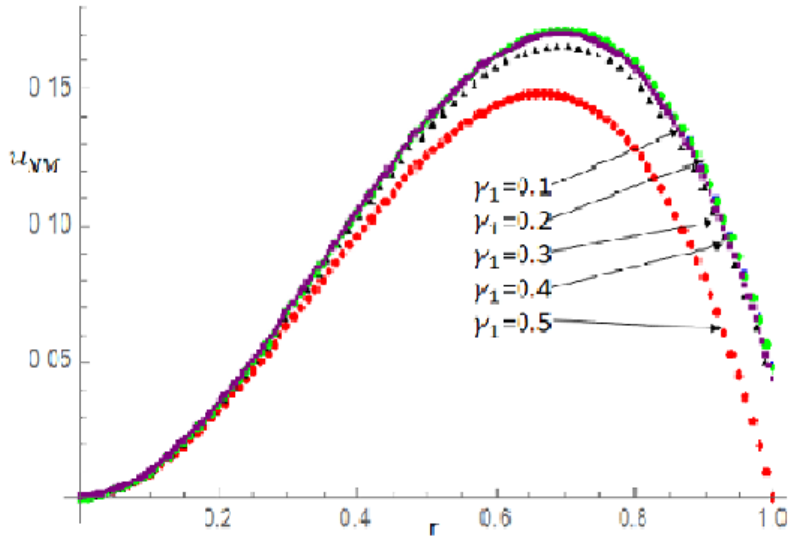

FIGURE 3.4: Numerical solution for different values of γ_1 for Equation Eq. (3.56) at $t = 0$.

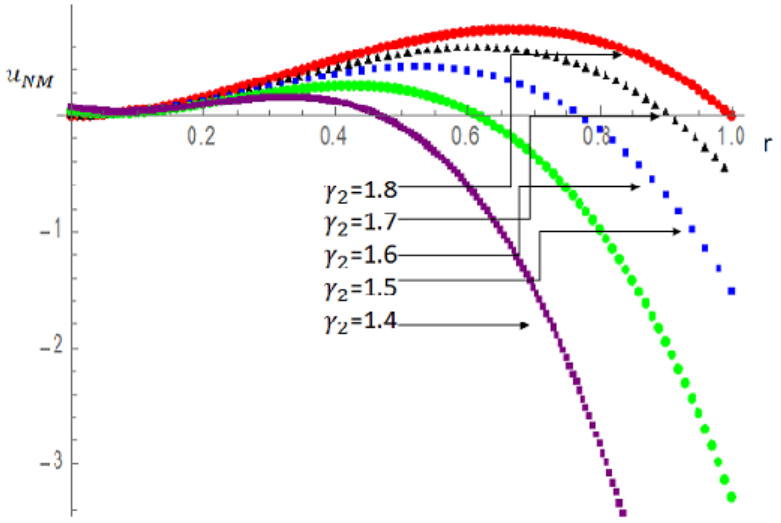

FIGURE 3.5: Numerical solution for different values of γ_2 for Equation Eq. (3.56) at $t = 1$.

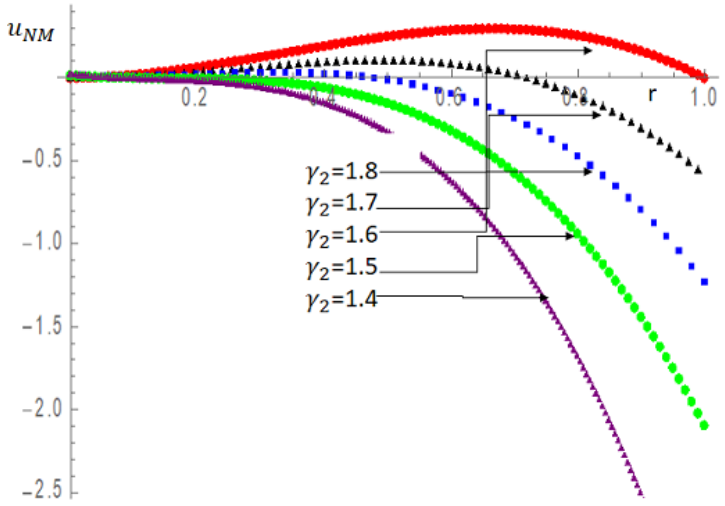

FIGURE 3.6: Numerical solution for different values of γ_2 for Eq. (3.56) at $t = 0.5$.

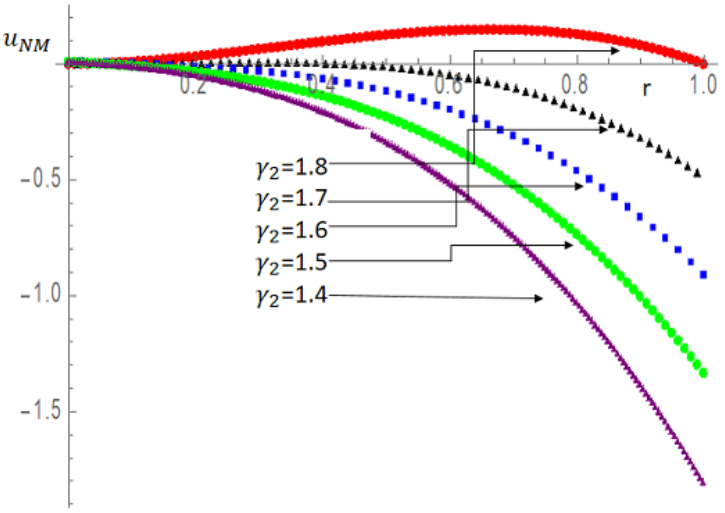

FIGURE 3.7: Numerical solution for different values of γ_2 for Eq. (3.56) at $t = 0$.

effect of noise by $u^{\delta}_{NM}(t, r)$. The obtained simulation results are demonstrated through Figs. (3.8-3.10) which represent the comparison between exact solution

$u(t,r)$, the approximate solution without noise $u^{\delta}_{NM}(t,r)$, and the approximate solution $u^{\delta}_{NM}(t,r)$ under the effect of random noise. It can be observed from (3.8-3.10) that the noisy solutions appear very close to the approximated solution without noise. This solution behavior establishes that the presented method is stable under the effect of random noise.

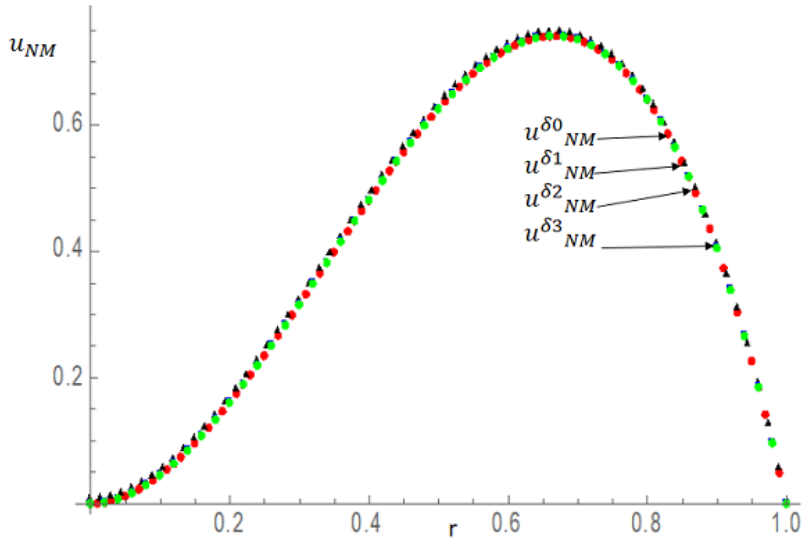

FIGURE 3.8: Numerical solution with different noise term for Eq. (3.56) at $t = 1$.

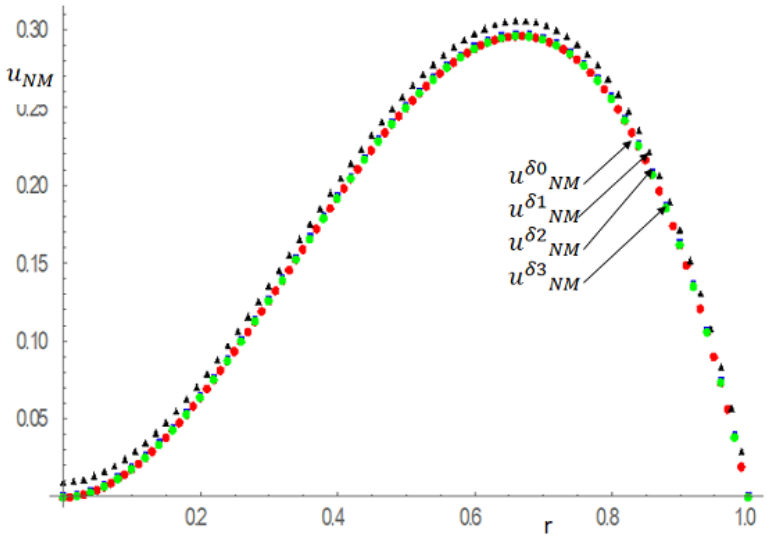

FIGURE 3.9: Numerical solution with different noise term for Eq. (3.56) at $t = 0.5$.

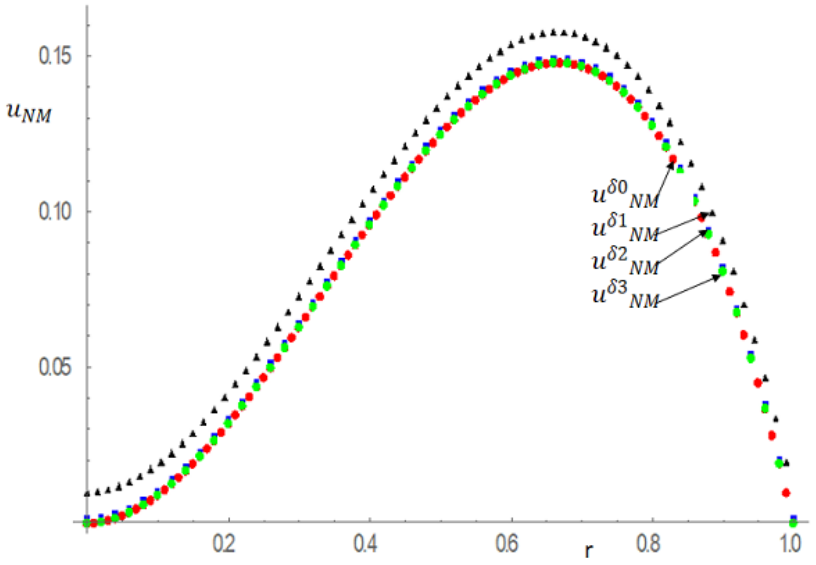

FIGURE 3.10: Numerical solution with different noise term for Eq. (3.56) at $t = 0$.

Example 3.7.2. Here, we consider a form of Eq. (3.5) as,

$$d_1(t,r)\int_a^t -\gamma_1(t-s)\frac{\delta u(s,r)}{\delta r}ds + \int_t^b -\gamma_1(s-t)\frac{\delta u(s,r)}{\delta r}\,ds$$
$$+d_2(t,r)\int_a^t -\gamma_2(t-s)\frac{\delta u(s,r)}{\delta r}ds + \int_t^b -\gamma_2(s-t)\frac{\delta u(s,r)}{\delta r}\,ds + u(t,r) = f(t,r). \tag{3.62}$$

with $p = q = 1,\ \gamma_1 = 1/2,\ \gamma_2 = 2/3,\ d_1(t,r) = 1,\ d_2(t,r) = -1/4$ and $f(t,r) = ((t^4(1-r)^3))/24 + (t^2 - (3-4t+t^4)/24)(r^3-1) + (3-4t+(2t)^4)(r^3-1)/72$. The exact solution in this case is $u(t,r) = t^2(r^3-1)$.

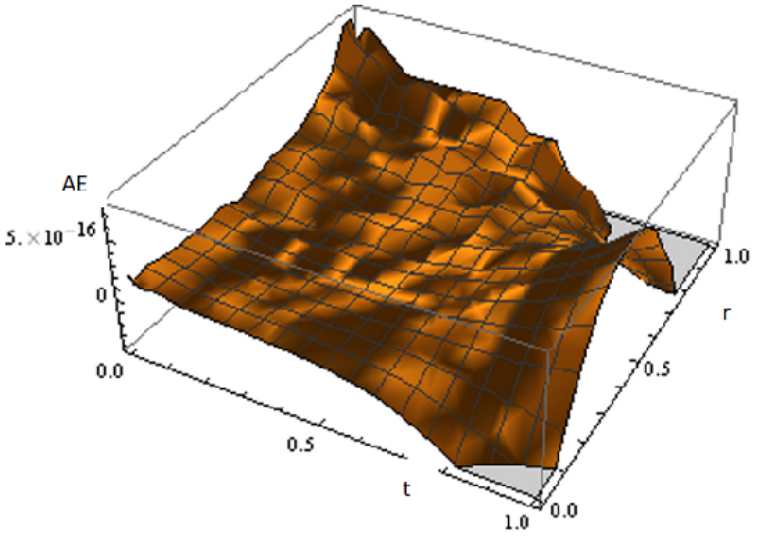

FIGURE 3.11: Plot of absolute numerical error for $N = 2,\ M = 3$ for Example (3.7.2).

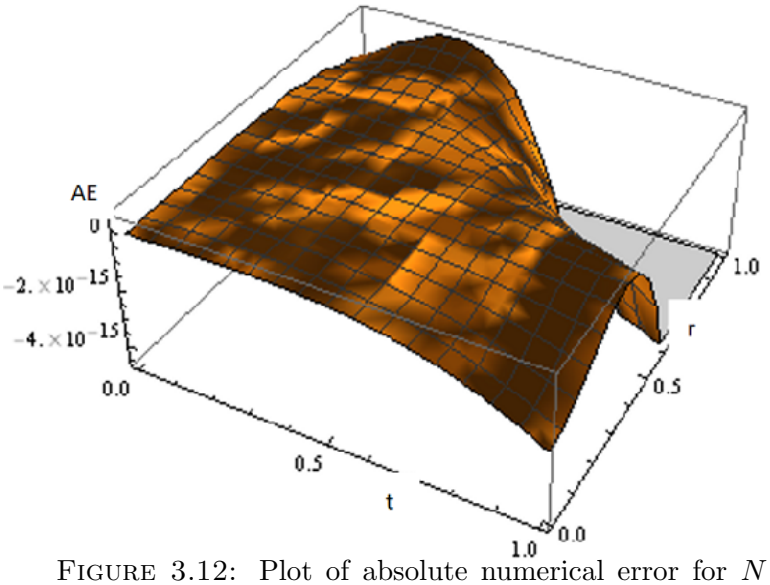

FIGURE 3.12: Plot of absolute numerical error for $N = M = 3$ for Example (3.7.2).

The solution of this example is approximated by the presented method and we observe that the obtained approximate solution has a well agreement with the exact solution. This problem is solved with different values of M and N and the obtained absolute errors are presented through Figs. (3.11-3.12). The maximum absolute errors at different points are listed in Table 3.5. The L_2 and L_∞ errors for this examples are presented in Table 3.6.

Fig. 3.12. Plot of absolute numerical error for $N = M = 3$ for Example 3.7.2. The numerical solutions for different values of γ_1 and γ_2 are obtained for this case and are shown through Figs. (3.13-3.15) and Figs. (3.16-3.18), respectively. It is observed that as we consider the value of γ_1 (or γ_2) close to $1/(2)(or 3/2)$, the approximate solution behaves like the exact solution known for $\gamma_1 = 1/2$ and $\gamma_2 = 3/2$. It is clear from the Figs. $(3.13 - 3.15)$ that numerical solutions converge to exact solution as the value γ_1 tends to $1/2$.

To verify the numerical stability for this test example, we perform the similar steps as done in case of example 1 and the obtained results are demonstrated through Figs. (3.19-3.20). Figs. (3.19-3.20) represent the comparison between exact solution $u(t,r)$, the approximate solution without noise $(u_{NM})(t,r)$, and the approximate solutions $(u_{NM})_n^{\delta}(t,r)$ with random noise δn.

TABLE 3.5: AE for Example (3.7.2).

(t,r)	$M=N=2$	$M=2,\ N=3$	$M=3,\ N=2$	$M=N=3$
(0.1,0.1)	2.99×10^{-5}	3.000×10^{-5}	3.122×10^{-17}	2.255×10^{-17}
(0.2,0.2)	5.551×10^{-17}	1.457×10^{-16}	1.387×10^{-17}	6.938×10^{-18}
(0.3,0.3)	2.774×10^{-4}	2.774×10^{-4}	2.775×10^{-17}	4.163×10^{-17}
(0.4,0.4)	0	0	0	2.775×10^{-17}
(0.5,0.5)	3.750×10^{-3}	3.750×10^{-3}	0	5.551×10^{-17}
(0.6,0.6)	1.728×10^{-3}	1.728×10^{-3}	1.110×10^{-16}	4.996×10^{-16}
(0.7,0.7)	5.145×10^{-2}	5.145×10^{-2}	0	2.331×10^{-15}
(0.8,0.8)	0.1228	0.1228	1.665×10^{-16}	7.494×10^{-15}
(0.9,0.9)	0.2551	0.2551	9.159×10^{-16}	1.931×10^{-14}
(1.0,1.0)	0.4798	0.4798	2.442×10^{-15}	4.302×10^{-14}

TABLE 3.6: L_2 and L_∞ errors for Example (3.7.2).

Errors	$M=N=2$	$M=2,\ N=3$	$M=3,\ N=2$	$M=N=3$
L_2 errors	0.5599	0.5599	2.616×10^{-15}	4.781×10^{-14}
L_∞ errors	0.4799	0.4799	2.442×10^{-15}	4.302×10^{-14}

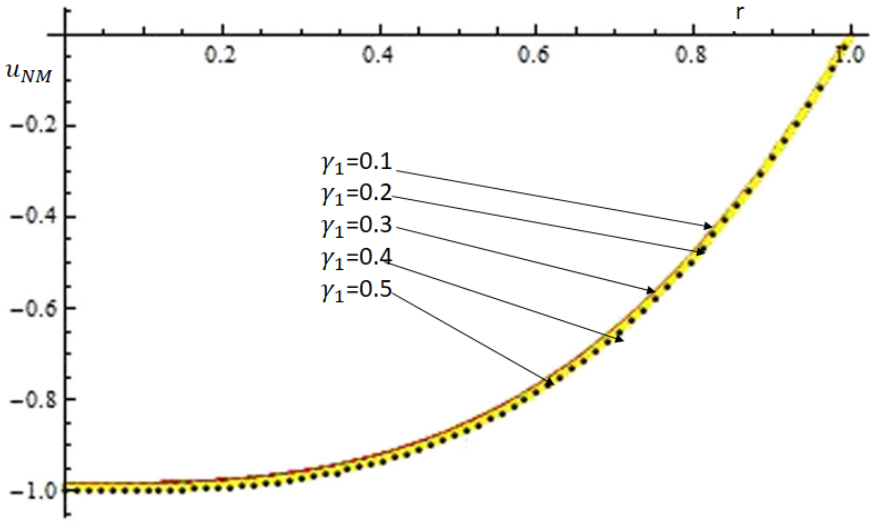

FIGURE 3.13: Numerical solution for different values of γ_1 for Example (3.7.2) at $t = 1$.

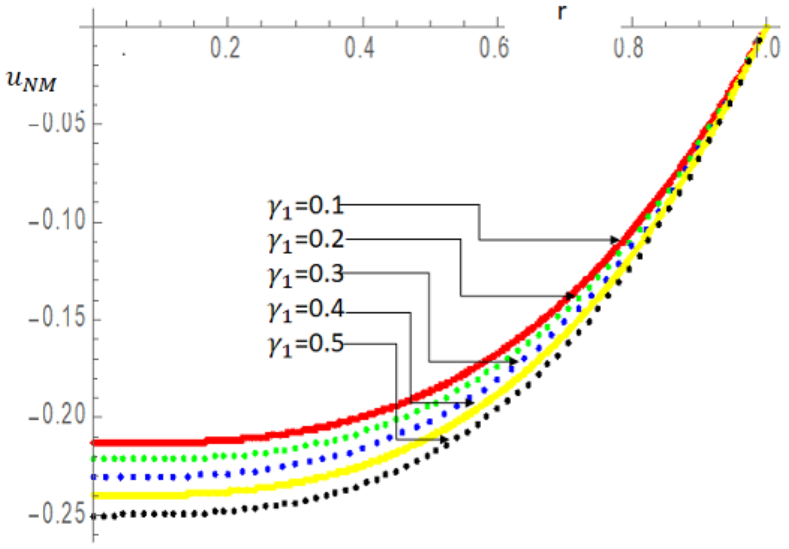

FIGURE 3.14: Numerical solution for different values of γ_1 for Example (3.7.2) at $t = 0.5$.

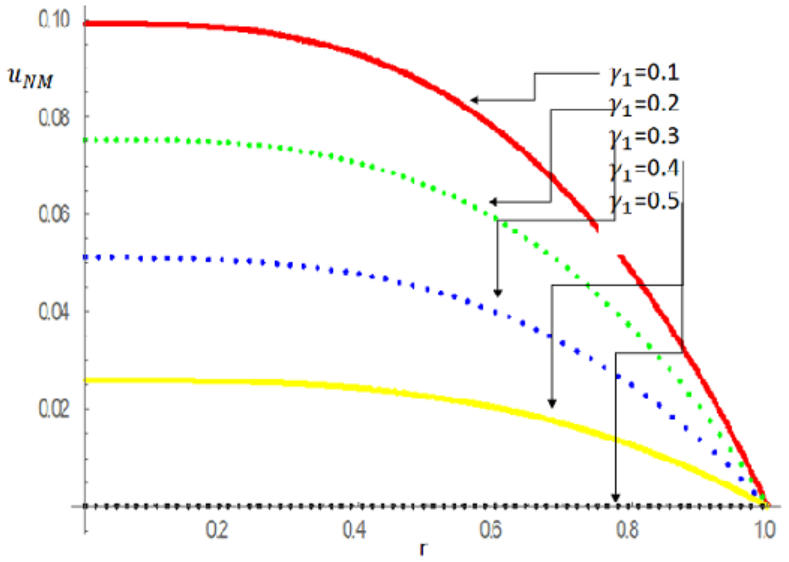

FIGURE 3.15: Numerical solution for different values of γ_1 for Example (3.7.2) at $t = 0$.

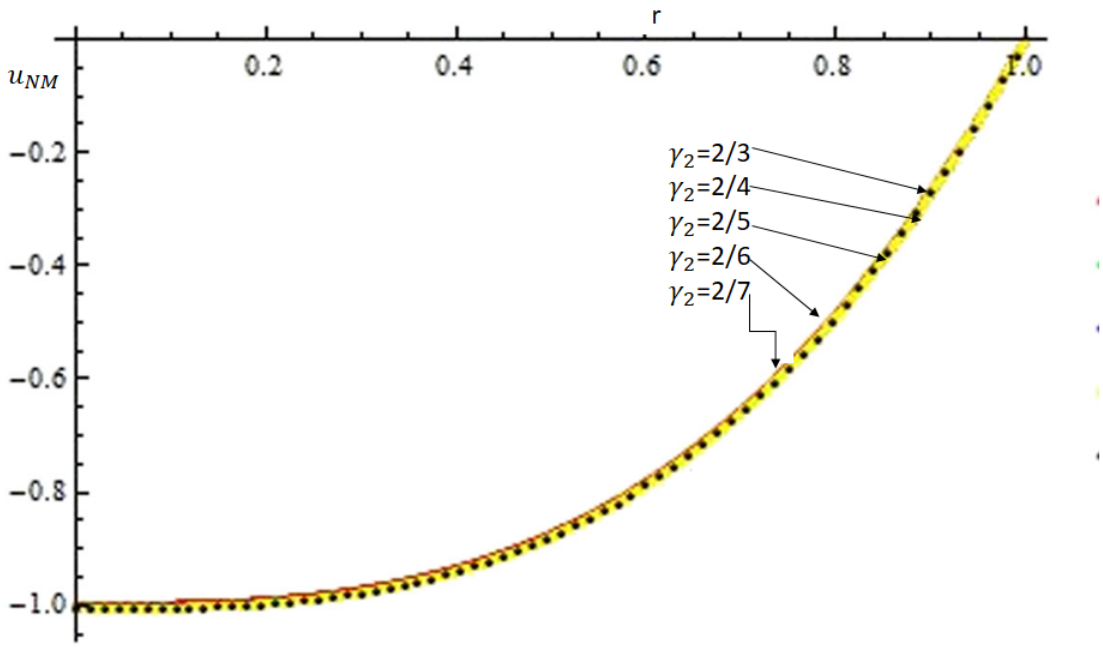

FIGURE 3.16: Numerical solution for different values of γ_2 for Example (3.7.2) at $t = 1$.

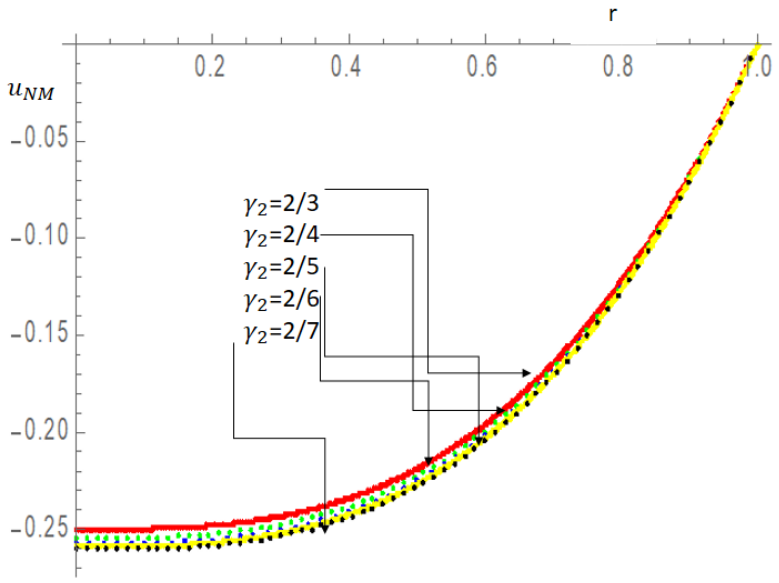

FIGURE 3.17: Numerical solution for different values of γ_2 for Example (3.7.2) at $t = 0.5$.

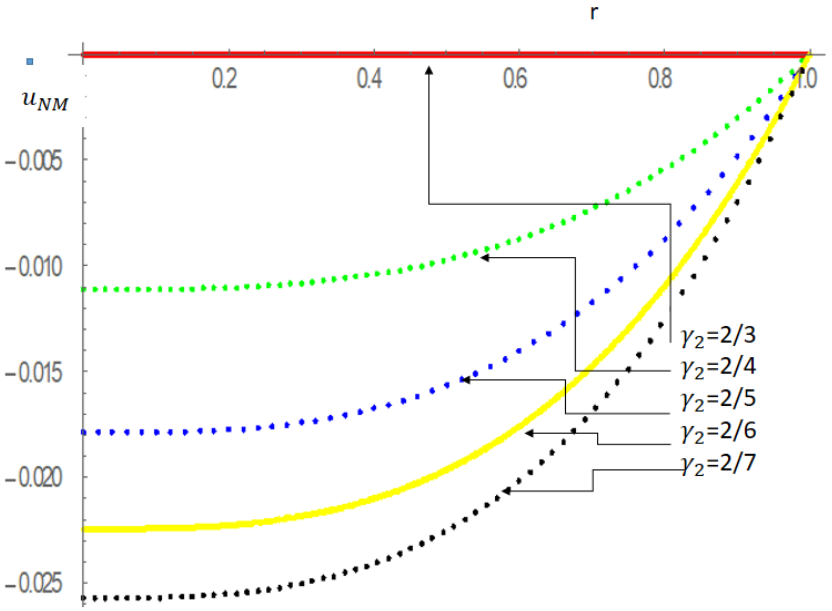

FIGURE 3.18: Numerical solution for different values of γ_2 for Example (3.7.2) at $t = 0$.

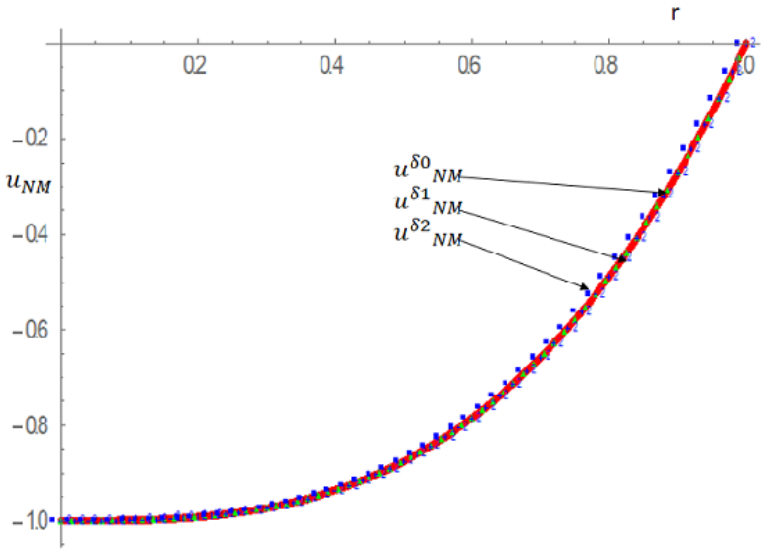

FIGURE 3.19: Numerical solution for different noise terms for Example (3.7.2) at

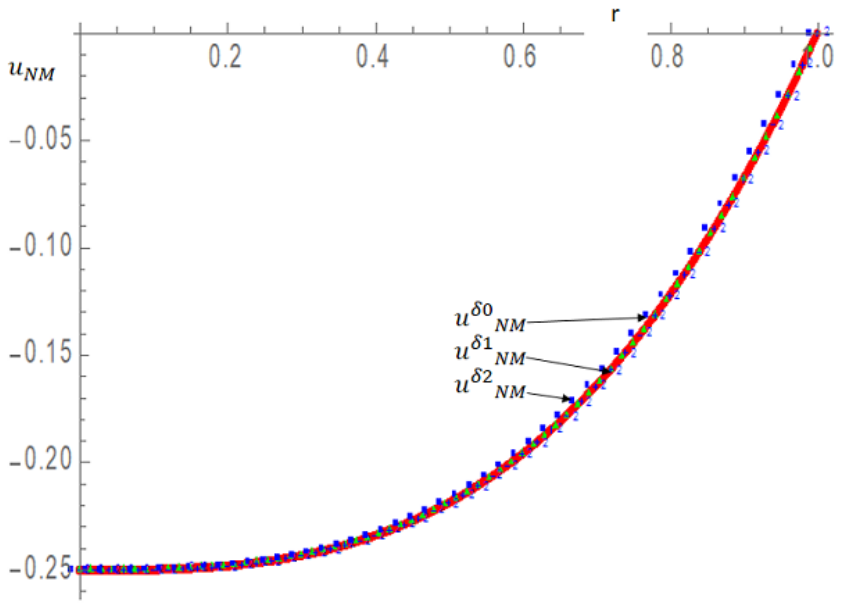

FIGURE 3.20: Numerical solution for different noise terms for Example (3.7.2) at $t = 0.5$.

3.8 Conclusions

We presented a generalized model of PIDEFO in this chapter. This model results the solution of several standard fractional models such as 1) linear space-time fractional reaction-diffusion equation (FRDE), 2) space-time fraction diffusion equations (STFDE) and 3) time fractional telegraph equations (TFTE), in special case. And thus, could be considered as the generalized PIDEFO model. The proposed method for the solution of the generalized PIDEFO is easy to apply and computationally efficient. This could be analyzed with the two examples discussed in the chapter, one with unknown solution (Example (3.7.1)) and second with known solutions (Example (3.7.2)). The approximated solution is also compared with a special case of Example (3.7.2) in which the solution is known. It was observed that the proposed method obtains good accuracy. We discussed only three special cases of the proposed model. Some other models may also be obtained as a case of the presented model and such studies will be presented in future.